

# Effect of emission on subnanosecond breakdown in a gas diode at low pressure

**E Kh Baksht<sup>1</sup>, S Ya Belomyttsev<sup>1</sup>, A G Burachenko<sup>1,2</sup>, A A Grishkov<sup>1</sup> and V A Shklyaev<sup>1,3</sup>**

<sup>1</sup>Institute of High Current Electronics, Russian Academy of Sciences, 2/3 Akademicheskoy Ave., 634055 Tomsk, Russia

<sup>2</sup>Tomsk State University, 36 Lenin Ave., 634050 Tomsk, Russia

<sup>3</sup>Institute of High Technology Physics, National Research Tomsk Polytechnic University, 30 Lenin Avenue, 634050 Tomsk, Russia

Email: beh@loi.hcei.tsc.ru

**Abstract.** The paper presents experimental and numerical research results on the operation of gas diode at low pressure. A high dispersion in the runaway electron beam current (from 20 to 100 A) with respect to the average one (~50 A) is observed for a tubular cathode with a working edge radius of 30  $\mu\text{m}$ , nitrogen pressure of 30 Torr, and an interelectrode gap of 6 mm. Numerical simulation data show that the low beam current (~20 A) is due to the early electron emission from the cathode (at the stage of low-voltage prepulse), in which the runaway electron beam is formed from the boundary of plasma layer developing early in the breakdown. The high beam current (~100 A) is due to the delayed electron emission from the cathode, which increases the diode voltage and the runaway electron beam current. In the latter case, the runaway electron beam is formed directly at the cathode.

## 1. Introduction

At present, many research papers dealing with generation of runaway electron beams in gas diodes with highly inhomogeneous electric field, considering the possibility to obtain such beams in various gases, at various pressures, the mechanisms of their generation and their parameters, depending on the interelectrode gap width as well as reporting about the cathode materials and their design, about the range of their possible applications, etc. have been published [1–4]. However, the generation stability of runaway electron beams, which is also very important, is reported only in [5, 6], in which general attention is paid to the onset of cathode operation in the steady-state mode (a conditioned cathode) without considering the dependence of beam current scattering on the gas diode parameters.

In experiments with the gas diodes, the current of runaway electron beam can differ greatly from pulse to pulse, under the same operating conditions. The stability of beam current is influenced by different factors. Our previous studies have shown that in nitrogen, at 30 Torr pressure, the duration of beam current is limited by the anode foil, which precludes the passage of electrons with the energies below threshold depending on the foil thickness [7, 8]. In this case, the beam current depends on the maximum voltage across the discharge gap (the breakdown voltage), and at the same voltage rise time, it depends, in fact, only on the emission characteristics determined by the state of the cathode surface.



Thus, the only factor that can be responsible for the beam current scattering under such conditions is the state of the cathode surface varying from pulse to pulse.

The objective of our experimental and numerical study was to investigate the effect of cathode emission on the generation stability and parameters of the runaway electron beam at the onset of the cathode to a steady-state mode. Clearly, the stability of beam parameters depends strongly on the voltage rise time, discharge chamber geometry, cathode design, gas pressure, and the state of cathode emitting surface. Whereas most of these parameters can be fixed or recorded by the diagnostic equipment, the state of cathode surface changes from shot to shot, and this can lead to an uncontrollable deviation of the runaway electron beam parameters. To study the influence of cathode emission on the runaway electron beam parameters, we considered the pulses, in which the rise time of incident voltage wave and the voltage amplitude were identical. It has been shown in [8], that the duration of beam current in nitrogen at 30 Torr pressure is limited by the foil, which separates the diode and the beam-measuring unit precluding the passage of electrons with the energies below 40 keV. That is, the beam current amplitude at such pressures depends only on the time of the onset of emission processes at the cathode.

## 2. Experiment

In our experiments, we used a SLEP-150 nanosecond generator connected to a transmission line filled with a transformer oil and to a gas diode (Figure 1). The anode was an Al foil of thickness 15  $\mu\text{m}$  (3) and a metal diaphragm of diameter 10 mm (2). The foil at its back was reinforced by grids of the total transparency 6.6 %, which in addition to reinforcement, provided attenuation of the beam current. The cathode (1) was a stainless steel tube of diameter 7.3 mm with a working edge 30  $\mu\text{m}$  thick. The amplitude of incident voltage wave in the transmission line was  $\sim 120$  kV with a rise time of  $\sim 250$  ps at a level of 0.1–0.9, and its FWHM with a matched load was  $\sim 1$  ns.

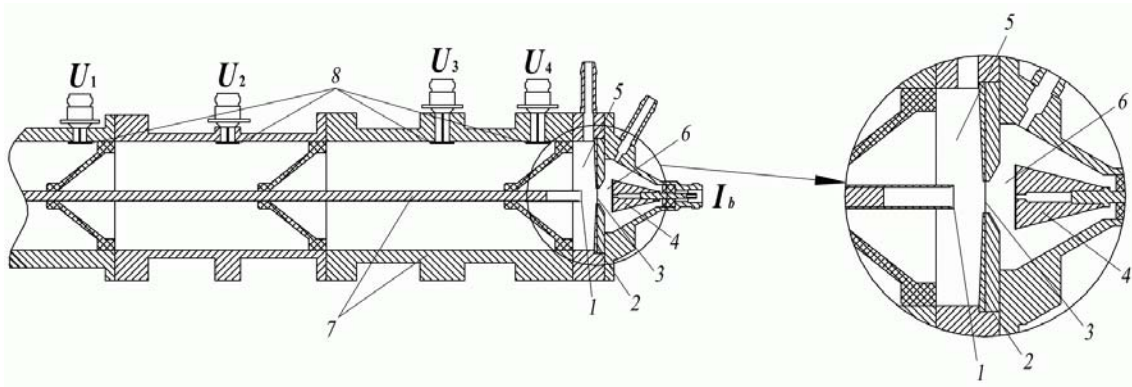


**Figure 1.** Transmission line and gas diode: 1 – cathode; 2 – diaphragm; 3 – Al foil; 4 – collector; 5 – gas diode; 6 – drift space; 7 – transmission line; 8 – capacitive dividers.

Figure 2 presents experimental data on the stability of the runaway electron beam current in a sample of 300 pulses. It is seen that the beam current ranges from 20 A to 100 A. Reasoning that all pulses were produced in a single series at a pressure of 30 Torr, it can be stated with confidence that it is the state of the emission surface, which influences the beam current under these conditions.

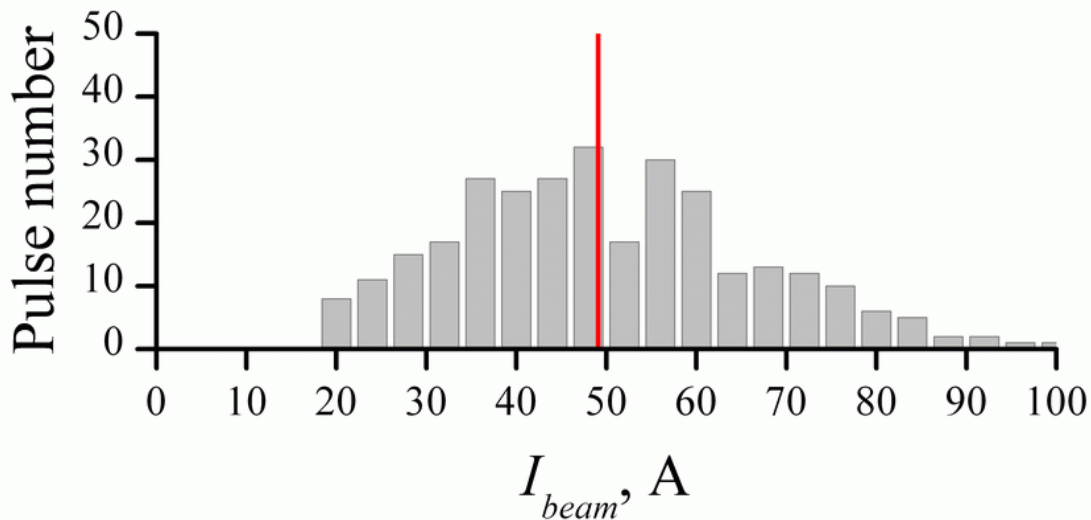


**Figure 2.** Histogram of the runaway electron beam current (gap width 6 mm, cathode rounding-off radius 30  $\mu\text{m}$ , nitrogen pressure 30 Torr).

### 3. Numerical simulation

Elucidating the effect of mission surface on the beam current amplitude, we simulated the breakdown developing under experimental conditions using the 2.5D (2D3V) axisymmetric PIC-code XOOPIC [9].

The computational domain included the diode with part of the transmission line and beam current measuring unit.

The emission was described using a model [8] covering both the field emission (the early breakdown stage) and the transition to explosive emission (the unlimited emission ability of cathode). The field emission was described by a modified Fowler–Nordheim formula for a cathode covered with microprotrusions having different amplification factors  $\beta$ . The above-mentioned formula includes an average amplification factor  $\langle\beta\rangle$  characterizing the state of its emission surface:

$$\langle j_{FN} \rangle(E) = \sqrt{\pi} AB^2 \varphi^2 \cdot \alpha^{3/2} \cdot \exp\left(-\frac{2}{\alpha}\right) \cdot \left\{1 + 2\sqrt{\frac{\alpha}{\pi}} + \frac{\alpha}{2}\right\}, \quad (1)$$

where  $\alpha = \sqrt{\frac{\langle\beta\rangle \cdot E_{macro}}{B\varphi^{3/2}}}$ ;  $\langle\beta\rangle$  is the average electric field amplification at the microprotrusions:

$$\langle\beta\rangle = 4-8 \quad [10].$$

The average current density estimated by formula (1) was multiplied by the total surface area  $I_{FN} = \langle j_{FN} \rangle \cdot S_C$  with calculation of the coefficient  $K$  for field-to-explosive emission transition:

$$\eta_t = \sum_t I_{FN}(t)^2 \cdot \Delta t, \quad (2)$$

$$K = \frac{\eta_t}{\eta_0}, \quad (3)$$

where  $\eta_0$  is equivalent to  $h$  being the specific action for explosion [11] but, unlike  $h$  calculated for the current density,  $\eta_0$  is selected for the total current from the cathode. This is because in the axisymmetric approximation used, we cannot describe individual microprotrusions, and experiments give only a general idea about emission properties of the cathode. The emission current was calculated by the expression

$$I_{em} = (1 - K) \cdot I_{FN} + K \cdot I_{ex} \quad (4)$$

where  $I_{ex}$  is the explosive emission current calculated using the Gauss theorem [9]. The electron emission from the cathode was specified by two parameters:  $\langle\beta\rangle$  for the onset of emission early in the breakdown and  $\eta_0$  for the time of field-to-explosive emission transition.

The emission parameters  $\langle\beta\rangle$  and  $\eta_0$  were varied so, that the beam current measured by the collector and the voltage at the third divider would coincide with their experimental values corresponding to the highest and lowest currents on the histogram in Figure 2, because the generation of runaway electrons and the breakdown dynamics at these values could differ greatly.

#### 4. Simulation results

Figure 3 presents experimental waveforms of the voltage from the divider  $U_3$  in the transmission line (grey solid curves) and the respective waveforms calculated by integrating the  $r$ -component of the electric field for the point of the divider position along the  $z$  axis (black solid curves). It is seen that the experimental data corresponding to the left (Figure 3a) and right (Figure 3b) branches of the beam current histogram in Figure 2 agree well with the calculations allowing, respectively, for the explosive emission by the Gauss law (Figure 3a) and for the field-to-explosive emission transition (Figure 3b). It is also seen from Figure 3 that according to integration of the electric field  $z$ -component from cathode to plane anode, the accelerating voltage across the diode (thin black curves) in two models of emission differs greatly.

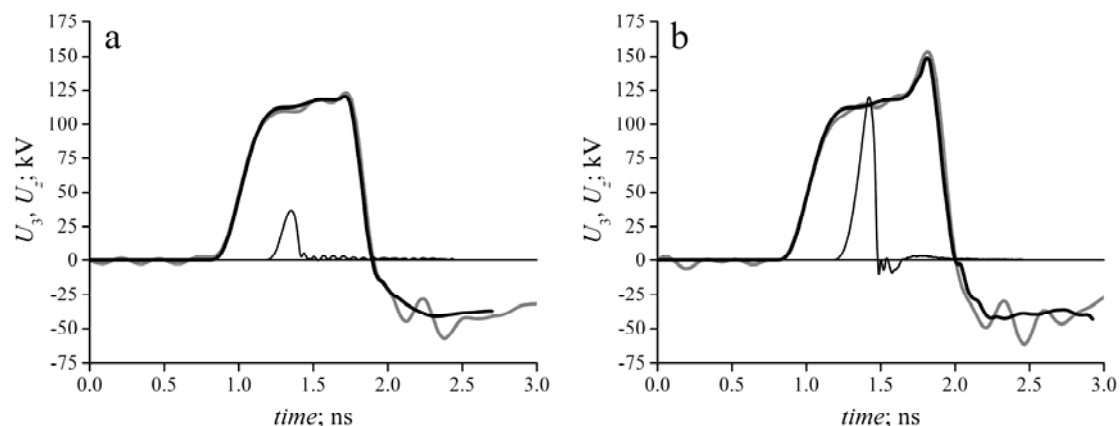


**Figure 3.** Experimental waveforms of the voltage from divider  $U_3$  (grey solid curves) for the left (a) and right (b) branches of the histogram in Figure 2 and respective calculated waveforms (black solid curves) for explosive emission (a) and for field-to-explosive emission transition (b);  $U_z$  – accelerating voltage across the diode (thin black curves).

The difference is due to different dynamics of breakdown and runaway electron generation in two emission models. In the model of explosive emission, the cathode becomes emitting almost immediately after arrival of the voltage when  $U_z$  is no greater than several kilovolts. Near the cathode, a plasma layer is formed (Figure 4a, 1.325 ns), giving rise to a runaway electron beam from its boundary and to a breakdown. Due to the early electron emission and pulsed breakdown, the maximum voltage  $U_z$  is not higher than 30 kV. In the model allowing for the field emission, we have a delay of an electron emission from the cathode and an increase in  $U_z$  to 125 kV, and the beam is formed directly at the cathode, in the region of a strong electric field. The runaway electron beam carries away a negative space charge, leaving only a positive space charge of ions resulting from the impact ionization of a neutral gas by electrons. Near the cathode, the cathode layer is formed (Figure 4b, 1.425 ns) with a potential fall reaching, by the estimates, tens of kilovolts (in contrast to the model

of explosive emission). During transition from the field to the explosive (unlimited) emission, the cathode layer disappears (Figure 4b, 1.45 ns).

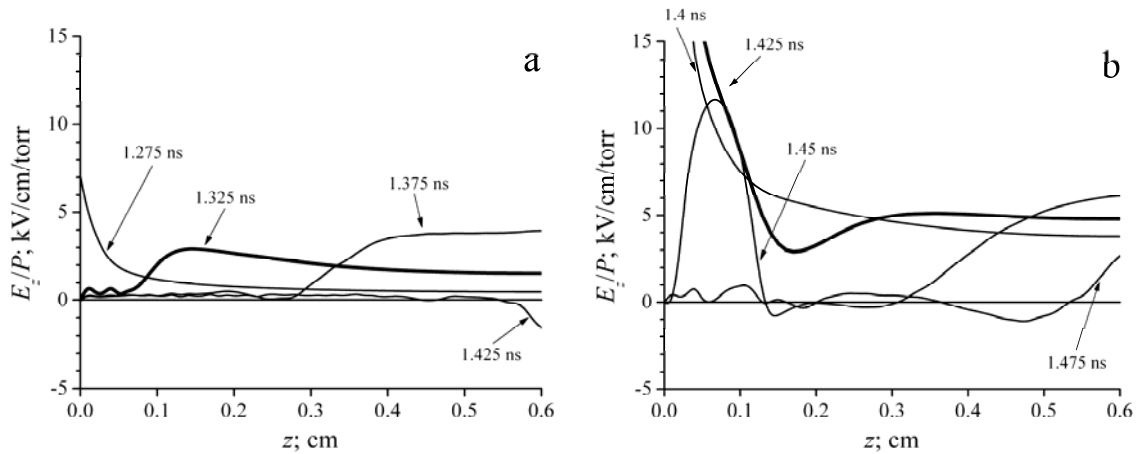


**Figure 4.** Distribution dynamics of the electric field  $z$ -component in the diode for explosive emission (a) and for field-to-explosive emission transition (b).

It is seen from Figure 4 that the electric field distributions in the diode for two emission models differ greatly, and hence, the beam currents in two cases differ greatly as well (Figure 5). In the model of explosive emission, the beam current at the collector is not higher than 20 A (Figure 5a), which corresponds to the left branch of the experimental histogram (Figure 2). In the model allowing for the field emission, the beam current reaches 110 A (Figure 5b), which is demonstrated by the right branch of the histogram (Figure 2).

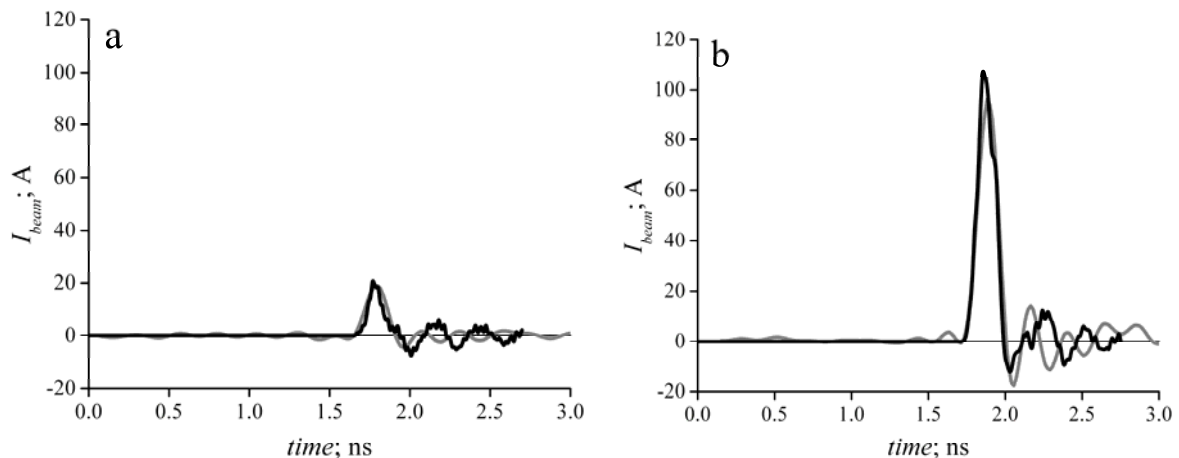


**Figure 5.** Experimental waveforms of the beam current (grey curves) and respective calculated waveforms (black curves) for explosive emission (a) and for field-to-explosive emission transition (b).

It should be noted that the calculated waveforms are timed. Our numerical simulation demonstrates that the two emission models give different points in time, at which runaway electrons are detected at the collector. In the model of explosive emission, the beam current at the collector peaks at 1.79 ns, and in the model allowing for the field emission, the beam current is delayed by almost 100 ps and its maximum falls on 1.88 ns.

## 5. Conclusion

Thus, we analyzed the scattering of experimental data in a large sample of pulses produced in a single series of experiments under the same conditions. The runaway electron beam current in the sample ranges from 20 to 100 A, and its deviation is associated mostly with the state of the emission surface of the cathode.

Our numerical simulation of the formation of a runaway electron beam and breakdown under conditions close to the experimental ones show that the modes of the processes and their dynamics differ in different models of emission.

## Acknowledgments

The work was supported by RFBR grants No. 14-02-00136 and No. 15-08-03983.

## References

- [1] *Runaway Electrons Preionized Diffuse Discharges* 2014 ed Tarasenko V F (New York: Nova Science Publishers, Inc.)
- [2] *Generation of runaway electrons and X-rays in high pressure discharges* 2015 ed Tarasenko V F (Tomsk, STT) In Russian
- [3] Babich L P, Loiko T V and Tsukerman V A 1990 *Phys. Usp.* **33** 521
- [4] Tarasenko V F and Yakovlenko S I 2004 *Phy. Usp.* **47** 887
- [5] Yalandin M I, Reutova A G, Ul'maskulov M R, Sharypov K A, Shpak V G, Shunailov S A, Klimov A I, Rostov V V and Mesyats G A 2009 *Tech. Phys. Lett.* **35** 804
- [6] Mesyats G A, Yalandin M I, Reutova A G, Sharypov K A, Shpak V G and Shunailov S A 2012 *Plasma Phys. Rep.* **38** 29
- [7] Baksht E Kh, Belomyttsev S Y, Burachenko A G, Grishkov A A, ShklyaeV V A and Tarasenko V F 2014 *Izv. Vyssh. Uchebn. Zaved. Fiz.* **57** 121 In Russian.
- [8] ShklyaeV V A, Baksht E Kh, Belomyttsev S Ya, Burachenko A G, Grishkov A A and Tarasenko V F 2015 *J. Appl. Phys.* **118** 213301
- [9] Verboncoeur J P, Langdon A B and Gladd N T 1995 *Comp. Phys. Commun.* **87** 199
- [10] Kozyrev A V, Korolev Y D, Mesyats G A 1987 *Sov. Phys. Tech. Phys.* **32** 34
- [11] Mesyats G A and Yalandin M I 2009 *Dokl. Phys.* **54** 63